

Integrated System of Fed Batch ABE Biosynthesis and Solvent Recovery by Pervaporation

ALI A. A. AL JANABI, TANASE DOBRE, OANA CRISTINA PARVULESCU*, TIBERIU DINU DANCUI, CLAUDIA PATRICHI

University Politehnica of Bucharest, Chemical and Biochemical Department, 1-3 Gheorghe Polizu Str., 011061, Bucharest, Romania

Anaerobic fermentation of glucose substrate by Clostridium acetobutylicum bacteria at 34-39 °C produces butanol, acetone, and ethanol solvents as metabolites. In the case of batch and fed batch bioreactors, the control of butanol concentration in the fermentation broth is recommended for diminishing its inhibitory effect on the bacterial system. Solvent recovery from batch or fed batch bioreactors by using an ultrafiltration-pervaporation system could be an efficient solution to improve the process performances. A mathematical model was developed in order to describe the dynamics of solvent production in an integrated system of fed batch fermentation and solvent recovery. Simulations performed under various operating conditions were used for optimizing the biosynthesis process, i.e., for maximizing the solvent production and minimizing the substrate concentration in the fermentation medium. Initial substrate concentration in the bioreactor, feed flow rate, feed substrate concentration, starting time of feed and ultrafiltration-pervaporation, surface area of ultrafiltration and pervaporation units were selected as process control variables.

Keywords: ABE fermentation, fed batch bioreactor, modelling, pervaporation, solvent recovery, ultrafiltration

Microbial synthesis of alcohol biofuels from renewable resources is a major research direction in biotechnology. Biobutanol has recently received more attention due to its potential to be an alternative fuel and fuel additive for gasoline and diesel engines [1-5]. Moreover, it is widely used as solvent, diluent, plasticizer, and chemical precursor [1-3]. Biobutanol is a characteristic metabolite of anaerobic fermentation of sugars and starch by *Clostridium* genus bacteria. *Clostridium acetobutylicum*, the most studied and manipulated strain, is able to use a broad variety of mono-, di-, and polysaccharides (e.g., glucose, fructose, mannose, galactose, xylose, arabinose, sucrose, lactose, dextrin, starch) as carbon source [1-3, 5-7].

Until the middle of the last century, batch ABE (acetone-butanol-ethanol) fermentation in the presence of *Clostridium acetobutylicum* was applied on an industrial scale to synthesize ABE solvents from food-based carbon sources, especially corn mash [2,3,7]. Clostridial fermentation is a two-phase process, where the bacteria produce acetic acid (AA), butyric acid (BA), CO₂, and H₂ (acidogenic phase) and further the acids are converted into ABE solvents (solventogenic phase) [1-3,5-7]. Temperatures of 34-39 °C and A:B:E mass ratio of 3:6:1 are typical for a batch fermentation process based on corn mash [2,4,7,8].

After the second world war, as effect of a significant increase in the food-based feedstocks, ABE production obtained by industrial clostridial fermentation became generally non-profitable compared to that derived from a petrochemical route [1-3,7]. Consequently, until the early 1960s, almost all ABE fermentation plants in the USA and Europe were replaced by petrochemical ones [2,3,7].

Nowadays, in the context of increasing demands for alternative fuels, of interest in using the renewable resources, as well as of the advances obtained in the field of biotechnology and engineering, there is an obvious

tendency towards the renewal of experimental and theoretical studies referring to ABE fermentation. In order to improve the fermentation performances, extensive researches have been done, including carbon source selection and treatment, batch/fed batch/continuous fermentation, and solvent recovery [1,2,5,7]. Clostridial fermentation performances are significantly influenced by the cost of carbon source (up to 79 % from the overall solvent production cost) and inhibitory effect of butanol on the bacterial system [2,6-8].

Low-cost wastes and by-products (e.g., molasses, wheat straws, corn stover, cheese whey, spoiled grains and fruits, fruit and wood waste) have been tested as carbon sources for ABE fermentation [2-4, 6,7]. Moreover, treatment methods of some feedstocks, especially lignocellulosic biomass, in order to obtain fermentescible sugars, have been established. Butanol inhibition results in low levels of solvent concentration (<20 g/L) and productivity (<0.3 g/(L×h)) in the fermentation broth [1-3,6,7]. Studies reported in the related literature have highlighted a diminishing of inhibitory effect by integrating the fermentation and solvent recovery. Liquid-liquid extraction [5,9-11], gas-stripping [12,13], adsorption [5,14], perstraction [15], and pervaporation [4, 16-25] are the most common methods used to recover the solvents from a fermentation medium. The application of a suitable recovery technique could heavily improve the solvent production and carbon source utilization.

The performances of an integrated system of ABE fermentation and solvent recovery by gas stripping were evaluated in our previous study [26]. This paper has aimed at modelling, simulation, and optimization the process of ABE biosynthesis coupled with solvent recovery by pervaporation. A mathematical model was developed to describe the dynamics of clostridial fermentation of a glucose substrate at 37 °C. Simulations were performed in

* email: oana.parvulescu@yahoo.com

order to determine the optimal conditions needed to maximize the solvent production and substrate utilization.

Model of ABE fermentation coupled with ultrafiltration and pervaporation

Physical model

The physical model describing ABE biosynthesis coupled with ultrafiltration and pervaporation is schematically illustrated in figure 1. The set-up consisted of a bioreactor (1), an ultrafilter (2), a pervaporation unit (3), a vacuum pump (4), a condenser (5), and a collector of volatiles (6). The ultrafiltration was needed in the system in order to avoid the membrane fouling in the pervaporation unit.

The bioreactor (1) worked sequentially, *i.e.* batch (B) mode in the first sequence, fed batch (FB) in the second one, and further fed batch coupled with ultrafiltration and volatile species pervaporation (FBUP). B operation mode was switched to FB at a time τ_F (h), when a volumetric flow rate F (m^3/h) of glucose substrate (S) at a concentration c_{SF} (kg/m^3) was fed into the bioreactor, whereas FB mode turned into FBUP at a time τ_{up} (h).

The process of ABE fermentation coupled with solvent recovery occurred as follows: (i) a volumetric flow rate (F_u) of fermentation broth left the bioreactor (1) and entered the ultrafilter (2), where the bacterial cells were retained in the retentate; (ii) the ultrafiltration retentate flow was recycled into the bioreactor and that of ultrafiltration permeate entered the pervaporation unit (3); (iii) the pervaporation retentate was recycled into the bioreactor, whereas the permeate vapour was condensed and further fed into the collector (6).

Simplifying assumptions and equations

Bioreactor

The specific growth rate of *Clostridium acetobutylicum* biomass (X) is estimated by eq. (1), where y is the dimensionless cellular RNA (ribonucleic acid) concentration, considered as a marker of the culture viability, and c_{RNA} is the cellular RNA concentration (c_{RNA}) at $\mu=0$ [5,26-28].

$$\mu = 0.56(y - 1) = 0.56 \left(\frac{c_{RNA}}{c_{RNA_{min}}} - 1 \right) \quad (1)$$

Total and partial mass balances in the bioreactor are expressed by eqs. (2)-(4), where V (m^3) is the bioreactor volume, F (m^3/h) the feed volumetric flow rate, F_u (m^3/h) the volumetric flow rate leaving the bioreactor and entering the ultrafiltration unit, F_r (m^3/h) the volumetric flow rate recycled into the bioreactor, c_i (kg/m^3) the concentration

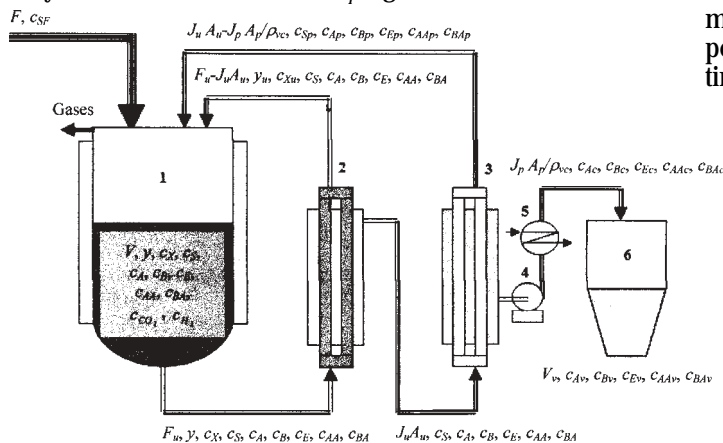


Fig. 1. Scheme of fed batch reactor coupled with ultrafiltration and volatile species pervaporation: (1) bioreactor, (2) ultrafilter, (3) pervaporation unit, (4) vacuum pump, (5) condenser, (6) collector of volatiles

of i species in the fermentation medium, c_{iF} (kg/m^3) the feed concentration of i species, c_{ir} (kg/m^3) the concentration of i species recycled into the bioreactor, R_i ($\text{kg}/(\text{m}^3 \times \text{h})$) the generation/consumption rate of i species, and τ (h) the time.

$$\frac{dV}{d\tau} = F - F_u + \sum_r F_r \quad (2)$$

$$\frac{d(Vy)}{d\tau} = VR_y + Fy_F - F_u y + \sum_r F_r y_r \quad (3)$$

$$\frac{d(Vc_i)}{d\tau} = VR_i + Fc_{iF} - F_u c_i + \sum_r F_r c_{ir} \quad (4)$$

$$i = X, S, A, B, E, AA, BA, \text{CO}_2, \text{H}_2$$

Ultrafiltration unit (UU)

Characteristic simplifying assumptions of UU were as follows: (i) ABE biosynthesis process was neglected due to the short residence time of ultrafiltration retentate; (ii) ultrafiltration permeate did not contain cellular material; (iii) solute species concentration was the same for ultrafiltration retentate and permeate, *i.e.*, $c_S, c_A, c_B, c_E, c_{AA}$ and c_{BA} .

Ultrafiltration permeate flux, J_u ($\text{m}^3/(\text{m}^2 \times \text{h})$), is an important operating parameter characterizing the UU. As the membrane fouling is neglected, it depends on the membrane type, trans membrane pressure, biomass concentration, and permeate viscosity [29-30]. In the presence of bacterial fouling, J_u will decrease in time as effect of formation of a gel layer on the membrane surface, leading to an increase in filtration resistance. According to membrane fouling model based on series resistances, the permeate flux is expressed by eq. (5), where η ($\text{kg}/(\text{m} \times \text{s})$) is the permeate viscosity, R_0 (m^{-1}) the initial membrane resistance, r_g ($\text{kg}/(\text{m}^3 \times \text{s})$) the specific resistance of gel layer, Δp (N/m^2) the trans membrane pressure, c_X (kg/m^3) the biomass concentration in the bioreactor, c_{Xg} (kg/m^3) the biomass concentration in the gel layer, and τ (h) the time [30, 31].

$$J_u = 3600 \left(\frac{1}{(\eta R_0)^2 + 3600 \frac{2r_g \Delta p c_X}{c_{Xg}} \tau} \right)^{0.5} \Delta p \quad (5)$$

For an UU based on a tubular ceramic membrane, the reported values for R_0 range from $2 \times 10^{13} \text{ m}^{-1}$ to $12 \times 10^{13} \text{ m}^{-1}$, depending on manufacture procedure [30-34]. Values of r_g/c_{Xg} between $3 \times 10^9 \text{ s}^{-1}$ and $8 \times 10^9 \text{ s}^{-1}$ can be selected if the velocity of retentate, containing no more than $5 \text{ kg}/\text{m}^3$ of cells, is over 2 m/s [30]. Variation of ultrafiltration permeate flux depending on trans membrane pressure and time is shown in figure 2.

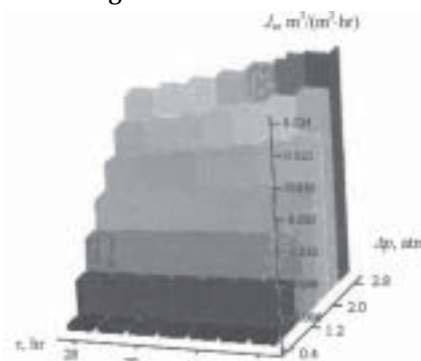


Fig. 2. Ultrafiltration permeate flux vs. trans membrane pressure and time ($R_0=410^{13} \text{ m}^{-1}$, $\eta=0.98 \times 10^{-3} \text{ kg}/(\text{m} \times \text{s})$, $r_g/c_{Xg}=5 \cdot 10^9 \text{ s}^{-1}$)

The concentration of cellular material in the retentate exiting the UU is given by the mass balances expressed by eqs. (6) and (7), where A_u (m²) is the ultrafiltration membrane surface area.

$$y_u = \frac{yF_u}{F_u - J_p A_p} \quad (6)$$

$$c_{xu} = \frac{c_x F_u}{F_u - J_p A_p} \quad (7)$$

Pervaporation unit (PU)-condenser system

Experimental data reported in the related literature [4,16-25] referring to membranes based on various polymers, e.g., polydimethylsiloxane (PDMS), polyvinyl alcohol (PVA), polytetrafluoroethylene (PTFE), were used in order to develop a simple model for the PU-condenser system. Accordingly, the total pervaporation flux, J_p (kg/(m²×h)), may be estimated at 37 °C depending on butanol concentration in the PU feed, c_B (kg/m³), using eq. (8). Moreover, the compositions of PU feed, c_i ($i=A, B, E, AA, BA$), and permeate leaving the condenser, c_{ic} are correlated by eqs. (9)-(14), where the subscript W refers to water. Due to zero value of its vapour pressure, the glucose substrate does not pass across the pervaporation membrane, consequently $c_{Sc} = 0$.

$$J_p = 0.915 + 0.036c_B^{1.2} \quad (8)$$

$$c_{Ac} = \begin{cases} 16c_A & c_A \leq 1 \text{ kg/m}^3 \\ 2.78 + 26.17c_A - 0.944c_A^2 & c_A > 1 \text{ kg/m}^3 \end{cases} \quad (9)$$

$$c_{Bc} = \begin{cases} 18c_B & c_B \leq 3 \text{ kg/m}^3 \\ 6.82 + 18.64c_B - 0.304c_B^2 & c_B > 3 \text{ kg/m}^3 \end{cases} \quad (10)$$

$$c_{Ec} = \begin{cases} 4c_E & c_E \leq 1 \text{ kg/m}^3 \\ 0.86 + 2.179c_E + 0.960c_E^2 & c_E > 1 \text{ kg/m}^3 \end{cases} \quad (11)$$

$$c_{AAc} = \begin{cases} 2c_{AA} & c_{AA} \leq 0.5 \text{ kg/m}^3 \\ 0.26 + 1.745c_{AA} + 0.281c_{AA}^2 & c_{AA} > 0.5 \text{ kg/m}^3 \end{cases} \quad (12)$$

$$c_{BAc} = \begin{cases} 2c_{BA} & c_{BA} \leq 0.5 \text{ kg/m}^3 \\ 0.07 + 1.231c_{BA} + 0.265c_{BA}^2 & c_{BA} > 0.5 \text{ kg/m}^3 \end{cases} \quad (13)$$

$$c_{Wc} = 952 - c_{Bc} - c_{Ac} - c_{Ec} - c_{AAc} - c_{BAc} \quad (14)$$

The density of condensed permeate, ρ_{vc} (kg/m³), was determined by eq. (15), where ρ_i ($i=A, B, E, AA, BA, W$) is the density of i species at 37 °C. The concentrations of i species ($i=S, A, B, E, AA, BA$) in the pervaporation retentate, c_{ip} (kg/m³), were calculated by Eqs. (16)-(21) based on characteristic mass balances of PU-condenser system inputs and outputs.

$$\frac{1}{\rho_{vc}} = \frac{1}{952} \left(\frac{c_{Bc}}{\rho_B} + \frac{c_{Ac}}{\rho_A} + \frac{c_{Ec}}{\rho_E} + \frac{c_{AAc}}{\rho_{AA}} + \frac{c_{BAc}}{\rho_{BA}} + \frac{c_{Wc}}{\rho_W} \right) \quad (15)$$

$$c_{Sp} = \frac{J_u A_u c_S - J_p A_p c_{Sc} / \rho_{vc}}{J_u A_u - J_p A_p / \rho_{vc}} \quad (16)$$

$$c_{Ap} = \frac{J_u A_u c_A - J_p A_p c_{Ac} / \rho_{vc}}{J_u A_u - J_p A_p / \rho_{vc}} \quad (17)$$

$$c_{Bp} = \frac{J_u A_u c_B - J_p A_p c_{Bc} / \rho_{vc}}{J_u A_u - J_p A_p / \rho_{vc}} \quad (18)$$

$$c_{Ep} = \frac{J_u A_u c_E - J_p A_p c_{Ec} / \rho_{vc}}{J_u A_u - J_p A_p / \rho_{vc}} \quad (19)$$

$$c_{AAp} = \frac{J_u A_u c_{AA} - J_p A_p c_{AAc} / \rho_{vc}}{J_u A_u - J_p A_p / \rho_{vc}} \quad (20)$$

$$c_{BAp} = \frac{J_u A_u c_{BA} - J_p A_p c_{BAc} / \rho_{vc}}{J_u A_u - J_p A_p / \rho_{vc}} \quad (21)$$

Collector of volatiles

The collector of volatiles was assumed as a perfectly mixed vessel characterized by eqs. (22)-(27), where V_v (m³) is the volume of collector liquid phase and c_{iv} (kg/m³) the concentration of i species ($i=A, B, E, AA, BA$) in the collector liquid.

$$\frac{dV_v}{d\tau} = \frac{J_p A_p}{\rho_{vc}} \quad (22)$$

$$\frac{dc_{Av}}{d\tau} = \frac{J_p A_p (c_{Ac} - c_{Av})}{\rho_{vc} V_v} \quad (23)$$

$$\frac{dc_{Bv}}{d\tau} = \frac{J_p A_p (c_{Bc} - c_{Bv})}{\rho_{vc} V_v} \quad (24)$$

$$\frac{dc_{Ev}}{d\tau} = \frac{J_p A_p (c_{Ec} - c_{Ev})}{\rho_{vc} V_v} \quad (25)$$

$$\frac{dc_{AAv}}{d\tau} = \frac{J_p A_p (c_{AAc} - c_{AAv})}{\rho_{vc} V_v} \quad (26)$$

$$\frac{dc_{BAv}}{d\tau} = \frac{J_p A_p (c_{BAc} - c_{BAv})}{\rho_{vc} V_v} \quad (27)$$

Integrated system of ABE fermentation and solvent recovery

According to eqs. (1)-(4), simplifying assumptions, and correlations for estimating the generation/consumption rate [28], characteristic total and partial mass balances of the bioreactor are expressed by eqs. (28)-(38). Mass balances of i gas species ($i=CO_2, H_2$) are given by eqs. (37) and (38), where c_{gi} (kg/m³) is the species concentration in the gas phase above the fermentation broth, k_{ia} (h⁻¹) the volumetric mass transfer coefficient in the liquid film, and k_{di} the distribution coefficient. Mass transfer and distribution coefficients may be determined based on the procedures presented in our previous paper [26]. The mathematical model describing ABE biosynthesis coupled with solvent recovery by ultrafiltration-pervaporation consists of eqs. (28)-(38) corresponding to the fermentation process in the bioreactor and eqs. (22)-(27) characterizing the solvent recovery in the collector of volatiles, where the parameters in eqs. (22)-(38) are calculated using eqs. (5)-(21).

$$\frac{dV}{d\tau} = F - J_p A_p / \rho_{vc} \quad (28)$$

$$\frac{dy}{d\tau} = \left[k_1 \frac{K_I}{K_I + c_B} c_S - 0.56(y-1) \right] y - \frac{F_u}{V} y + \frac{F_u - J_u A_u}{V} y_u \quad (29)$$

$$\frac{dc_x}{d\tau} = 0.56(y-1)c_x - k_2 c_B c_x - \frac{F_u}{V} c_x + \frac{F_u - J_u A_u}{V} c_{xu} - \frac{c_x}{V} \frac{dV}{d\tau} \quad (30)$$

$$\frac{dc_S}{d\tau} = -k_3 c_S c_x - k_4 \frac{c_S}{K_S + c_S} c_x + \frac{F}{V} c_{SF} - \frac{J_u A_u}{V} c_S + \frac{J_u A_u - J_p A_p / \rho_{vc}}{V} c_{Sp} - \frac{c_S}{V} \frac{dV}{d\tau} \quad (31)$$

$$\frac{dc_{BA}}{d\tau} = k_5 \frac{K_I}{K_I + c_B} c_S c_x - k_6 \frac{c_{BA}}{K_{BA} + c_{BA}} c_x - \frac{J_u A_u}{V} c_{BA} + \frac{J_u A_u - J_p A_p / \rho_{vc}}{V} c_{BAp} - \frac{c_{BA}}{V} \frac{dV}{d\tau} \quad (32)$$

$$\frac{dc_B}{d\tau} = k_7 c_S c_X - 0.8 \left(k_5 \frac{K_I}{K_I + c_B} c_S c_X - k_6 \frac{c_{BA}}{K_{BA} + c_{BA}} c_X \right) - \frac{J_u A_u}{V} c_B + \frac{J_p A_p - J_p A_p / \rho_{vc}}{V} c_{Bp} \quad (33)$$

$$\frac{dc_{AA}}{d\tau} = \left(k_8 \frac{K_I}{K_I + c_B} - k_9 \frac{c_{AA}}{K_{AA} + c_{AA}} \right) \frac{c_S}{K_S + c_S} c_X - \frac{J_u A_u}{V} c_{AA} + \frac{J_p A_p - J_p A_p / \rho_{vc}}{V} c_{AAp} - \frac{c_{AA}}{V} \frac{dV}{d\tau} \quad (34)$$

$$\begin{aligned} \frac{dc_A}{d\tau} = & k_{10} \frac{c_S}{c_S + k_S} c_X - 0.5 \left(k_8 \frac{K_I}{K_I + c_B} - k_9 \frac{c_{AA}}{K_{AA} + c_{AA}} \right) \frac{c_S}{K_S + c_S} c_X - \frac{J_u A_u}{V} c_A + \\ & + \frac{J_p A_p - J_p A_p / \rho_{vc}}{V} c_{Ap} - \frac{c_A}{V} \frac{dV}{d\tau} \end{aligned} \quad (35)$$

$$\frac{dc_E}{d\tau} = k_{11} \frac{c_S}{K_S + c_S} c_X - \frac{J_u A_u}{V} c_E + \frac{J_p A_p - J_p A_p / \rho_{vc}}{V} c_{Ep} - \frac{c_E}{V} \frac{dV}{d\tau} \quad (36)$$

$$\frac{dc_{CO_2}}{d\tau} = k_{12} \frac{c_S}{K_S + c_S} c_X - k_{ICO_2} a (c_{CO_2} - k_{dCO_2} c_{gCO_2}) - \frac{c_{CO_2}}{V} \frac{dV}{d\tau} \quad (37)$$

$$\frac{dc_{H_2}}{d\tau} = k_{13} \frac{c_S}{K_S + c_S} c_X + k_{14} c_S c_X - k_{IH_2} a (c_{H_2} - k_{dH_2} c_{gH_2}) - \frac{c_{H_2}}{V} \frac{dV}{d\tau} \quad (38)$$

Model restrictions corresponding to B, FB, and FBUP operating are given by Eqs. (39)-(41). Table 1 contains characteristic values of kinetic ($k_1 \dots k_{14}$) and Monod (K_I, K_S, K_{AA} , and K_{BA}) constants characterizing the ABE biosynthesis model.

$$\tau = 0 : \begin{cases} V = V_0, \dot{V}_v = 0 \\ y = y_0, c_X = c_{X,0}, c_S = c_{S,0}, c_B = c_{B,0}, c_A = c_{A,0}, c_E = c_{E,0}, c_{AA} = c_{AA,0}, c_{BA} = c_{BA,0} \\ c_{CO_2} = c_{CO_2,0}, c_{H_2} = c_{H_2,0}, c_{gCO_2} = c_{gCO_2,0} = 0, c_{gH_2} = c_{gH_2,0} = 0 \\ c_{Bv} = c_{Bv,0} = 0, c_{Av} = c_{Av,0} = 0, c_{Ev} = c_{Ev,0} = 0, c_{AAv} = c_{AAv,0} = 0, c_{BAv} = c_{BAv,0} = 0 \end{cases} \quad (39)$$

$$\tau < \tau_F : F = F(\tau) = 0, \tau \geq \tau_F : F = F(\tau) = \varepsilon V_0 \quad (40)$$

$$\tau < \tau_{UP} : F_u = F_u(\tau) = 0, \tau \geq \tau_{UP} : F_u = F_u(\tau) = F = \varepsilon V_0 \quad (41)$$

Optimization case

The mathematical model was applied to solve an optimization case consisting in maximizing the final ABE production (F_{opt} defined by eq. (42)) and minimizing the substrate concentration in the final bioreactor broth (c_{Sf}). This problem required to obtain the optimal values of initial substrate concentration in the bioreactor fermentation broth (c_{S0}), feed volumetric flow rate (F), substrate concentration in the bioreactor feed (c_{SF}), starting time of feed (τ_F) and ultrafiltration-pervaporation (τ_{UP}), surface area of ultrafiltration (A_u) and pervaporation (A_p) units. Positive terms in the objective function F_{opt} refer to carbon content of final (f) ABE production in the bioreactor and collector of volatiles, whereas negative terms include carbon mass contained in the final amount of X, S, AA, and BA, as well as that corresponding to the initial ABE amount in the bioreactor broth. Term coefficients in eq. (42) were calculated as ratio between the mass of carbon atoms in i species molecule (g_C/mol) and i species molecular mass (g/mol).

$$\begin{aligned} F_{opt}(c_{S,0}, F, c_{SF}, \tau_F, A_p, A_u, \tau_{UP}) = & \frac{0.65c_{Bvf}V_{vf}}{V_f} + \frac{0.62c_{Avf}V_{vf}}{V_f} + \frac{0.52c_{Evf}V_{vf}}{V_f} + \\ & + 0.65 \left(c_{Bf} - \frac{V_0 c_{B,0}}{V_f} \right) + 0.62 \left(c_{Af} - \frac{V_0 c_{A,0}}{V_f} \right) c_{Af} + 0.52 \left(c_{Ef} - \frac{V_0 c_{E,0}}{V_f} \right) c_{Ef} - \\ & - 0.48c_{Xf} - 0.40c_{Sf} - 0.40c_{AAf} - 0.55c_{BAf} - \frac{0.40c_{AAvf}V_{vf}}{V_f} - \frac{0.55c_{BAvf}V_{vf}}{V_f} \end{aligned} \quad (42)$$

Parameter	Unit	Value	Parameter	Unit	Value
k_1	$m^3/(kg \cdot hr)$	0.0090	k_{10}	hr^{-1}	0.1558
k_2	$m^3/(kg \cdot hr)$	0.0008	k_{11}	hr^{-1}	0.0258
k_3	$m^3/(kg \cdot hr)$	0.0255	k_{12}	hr^{-1}	0.6139
k_4	hr^{-1}	0.6764	k_{13}	hr^{-1}	0.0185
k_5	$m^3/(kg \cdot hr)$	0.0136	k_{14}	$m^3/(kg \cdot hr)$	0.00013
k_6	hr^{-1}	0.1170	K_I	kg/m^3	0.8330
k_7	$m^3/(kg \cdot hr)$	0.0113	K_S	kg/m^3	2.0
k_8	hr^{-1}	0.7150	K_{AA}	kg/m^3	0.5
k_9	hr^{-1}	0.1350	K_{BA}	kg/m^3	0.5

Table 1
KINETIC AND MONOD CONSTANTS FOR ABE BIOSYNTHESIS [28]

Results and discussions

A two-stage procedure was adopted in order to solve the optimization case. In the first stage, characteristic objective functions F_{opt} and c_{Sf} of B-FB bioreactor were optimizing considering $c_{S,0}$, $F = \varepsilon V_0$, c_{SF} and τ_F as process factors (manipulated parameters). Optimal values of

process factors obtained in the first stage were further used as input constant parameters for the second optimization stage, where objective functions corresponding to a B-FB-FBUP system, i.e., $F_{opt}(A_u, A_p, \tau_{UP})$ and $c_{Sf}(A_u, A_p, \tau_{UP})$, were optimized.

In order to solve the optimization problem for B-FB bioreactor, a second order (quadratic) response surface (SORS) model with 4 factors was applied [35]. Minimal, central (within the centre of experimental plan), and maximal levels of process factors, as well as values of fixed parameters are summarized in table 2. Table 3 contains the experimentation matrix corresponding to a SORS model, where the dimensionless values of process factors, x_j ($j=1...4$), were determined by eq. (43) and those of x'_j by eq. (44). Characteristic regression coefficients of SORS statistical models described by eqs. (45) and (46) were calculated using eqs. (47)-(50).

$$x_j = \frac{z_j - z_{j,C}}{\Delta z_j} = \frac{z_j - \frac{z_{j,max} + z_{j,min}}{2}}{\frac{z_{j,max} - z_{j,min}}{2}}, j=1...4 \quad (43)$$

$$x'_j = x_j^2 - \frac{\sum_{i=1}^{25} x_{ji}^2}{25} = x_j^2 - \overline{x_j^2}, j=1...4 \quad (44)$$

$$y_1 = F_{opt,I}(x_1, x_2, x_3, x_4) = \beta_{0,1} + \sum_{j=1}^4 \beta_{j,1} x_j + \sum_{j=1}^4 \sum_{l=1, l>j}^4 \beta_{j,l,1} x_j x_l + \sum_{j=1}^4 \beta_{j,j,1} x_j^2 \quad (45)$$

$$y_2 = c_{SF,I}(x_1, x_2, x_3, x_4) = \beta_{0,2} + \sum_{j=1}^4 \beta_{j,2} x_j + \sum_{j=1}^4 \sum_{l=1, l>j}^4 \beta_{j,l,2} x_j x_l + \sum_{j=1}^4 \beta_{j,j,2} x_j^2 \quad (46)$$

$$\beta_{0,k} = \frac{\sum_{i=1}^{25} y_{ki}}{25}, k=1, 2 \quad (47)$$

$$\beta_{j,k} = \frac{\sum_{i=1}^{25} x_{ji} y_{ki}}{\sum_{i=1}^{25} x_{ji}^2}, j=1...4 \text{ and } k=1, 2 \quad (48)$$

Type	Name	Symbol	Value	Unit	
Manipulated	Glucose substrate concentration	$c_{S,0}$	$z_{1,min}$	50	kg/m ³
			$z_{1,C}$	100	
			$z_{1,max}$	150	
	Feed flow rate	F	$z_{2,min}$	0.02V ₀	m ³ /hr
			$z_{2,C}$	0.05V ₀	
			$z_{2,max}$	0.08V ₀	
	Feed glucose concentration	c_{SF}	$z_{3,min}$	100	kg/m ³
			$z_{3,C}$	150	
			$z_{3,max}$	200	
	Feed starting time	τ_F	$z_{4,min}$	5	hr
			$z_{4,C}$	10	
			$z_{4,max}$	15	
Fixed	Biomass concentration	$c_{X,0}$	1.2	kg/m ³	
	Butanol concentration	$c_{B,0}$	0.5	kg/m ³	
	Acetone concentration	$c_{A,0}$	0.81	kg/m ³	
	Ethanol concentration	$c_{E,0}$	0.24	kg/m ³	
	Butyric acid concentration	$c_{BA,0}$	4.78	kg/m ³	
	Acetic acid concentration	$c_{AA,0}$	3.68	kg/m ³	
	Carbon dioxide concentration	$c_{CO_2,0}$	0	kg/m ³	
	Hydrogen concentration	$c_{H_2,0}$	0	kg/m ³	
	Marker concentration	y_0	1.2	-	
Batch reactor volume	V_0	30	m ³		

Table 2
INPUT PARAMETERS FOR ABE
BIOSYNTHESIS IN B-FB SYSTEM

Table 3
SIMULATION MATRIX FOR ABE BIOSYNTHESIS IN B-FB SYSTEM USING SECOND-ORDER RESPONSE SURFACE (SORS) MODEL

No.	x_1	x_2	x_3	x_4	x'_1	x'_2	x'_3	x'_4	$x_1 x_2$	$x_1 x_3$	$x_1 x_4$	$x_2 x_3$	$x_2 x_4$	$x_3 x_4$	$y_1 = F_{opt,I}$ (kg _c /m ³)	$y_2 = c_{SF,I}$ (kg _s /m ³)
1	+1	+1	+1	+1	0.2	0.2	0.2	0.2	+1	+1	+1	+1	+1	+1	14.269	54.151
2	-1	-1	+1	+1	0.2	0.2	0.2	0.2	+1	-1	-1	-1	-1	+1	23.192	22.501
3	+1	-1	-1	+1	0.2	0.2	0.2	0.2	-1	-1	+1	+1	-1	-1	18.243	5.098
4	-1	+1	-1	+1	0.2	0.2	0.2	0.2	-1	+1	-1	-1	+1	-1	13.909	2.343
5	+1	-1	+1	-1	0.2	0.2	0.2	0.2	-1	+1	-1	-1	+1	-1	20.994	36.608
6	-1	+1	+1	-1	0.2	0.2	0.2	0.2	-1	-1	+1	+1	-1	-1	19.953	43.845
7	+1	+1	-1	-1	0.2	0.2	0.2	0.2	+1	-1	-1	-1	-1	+1	16.491	1.799
8	-1	-1	-1	-1	0.2	0.2	0.2	0.2	+1	+1	+1	+1	+1	+1	13.811	1.668
9	+1	-1	+1	+1	0.2	0.2	0.2	0.2	-1	+1	+1	-1	-1	+1	17.736	39.963
10	-1	+1	+1	+1	0.2	0.2	0.2	0.2	-1	-1	-1	+1	+1	+1	19.111	41.682
11	+1	+1	-1	+1	0.2	0.2	0.2	0.2	+1	-1	-1	-1	+1	-1	15.553	3.855
12	-1	-1	-1	+1	0.2	0.2	0.2	0.2	+1	+1	+1	+1	-1	-1	13.089	2.465
13	+1	+1	+1	-1	0.2	0.2	0.2	0.2	+1	+1	-1	+1	-1	-1	14.869	54.151
14	-1	-1	+1	-1	0.2	0.2	0.2	0.2	+1	-1	+1	-1	+1	-1	23.735	22.16
15	+1	-1	-1	-1	0.2	0.2	0.2	0.2	-1	-1	-1	+1	+1	+1	18.938	2.729
16	-1	+1	-1	-1	0.2	0.2	0.2	0.2	-1	+1	+1	-1	-1	+1	14.622	1.517
17	0	0	0	0	-0.8	-0.8	-0.8	-0.8	0	0	0	0	0	0	22.029	14.324
18	1.414	0	0	0	1.2	-0.8	-0.8	-0.8	0	0	0	0	0	0	20.241	21.117
19	-1.414	0	0	0	1.2	-0.8	-0.8	-0.8	0	0	0	0	0	0	21.636	11.027
20	0	1.414	0	0	-0.8	1.2	-0.8	-0.8	0	0	0	0	0	0	22.359	15.207
21	0	-1.414	0	0	-0.8	1.2	-0.8	-0.8	0	0	0	0	0	0	22.258	5.556
22	0	0	1.414	0	-0.8	-0.8	1.2	-0.8	0	0	0	0	0	0	16.097	56.412
23	0	0	-1.414	0	-0.8	-0.8	1.2	-0.8	0	0	0	0	0	0	10.591	0.954
24	0	0	0	1.414	-0.8	-0.8	-0.8	1.2	0	0	0	0	0	0	19.303	17.892
25	0	0	0	-1.414	-0.8	-0.8	-0.8	1.2	0	0	0	0	0	0	23.847	12.084

$$\beta_{jj,k} = \frac{\sum_{i=1}^{25} x_{ji} y_{ki}}{\sum_{i=1}^{25} (x_{ji})^2}, j=1...4 \text{ and } k=1, 2 \quad (49)$$

$$\beta_{jl,k} = \frac{\sum_{i=1}^{25} x_{ji} x_{li} y_{ki}}{\sum_{i=1}^{25} (x_{ji} x_{li})^2}, j, l=1...4, j < l, \text{ and } k=1, 2 \quad (50)$$

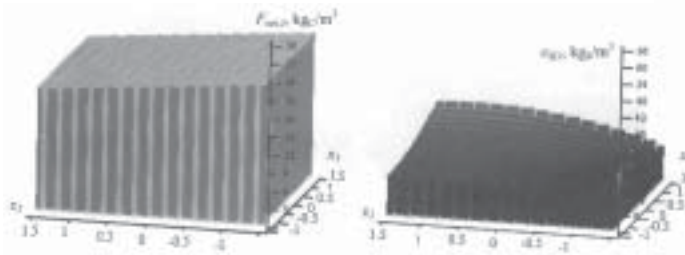


Fig. 3. $F_{opt,I}$ and $c_{Sf,I}$ vs. x_1 and x_2 ($x_3 = x_4 = 0$)

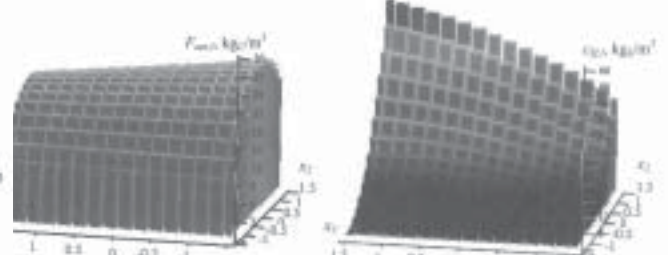


Fig. 6. $F_{opt,I}$ and $c_{Sf,I}$ vs. x_2 and x_3 ($x_1 = x_4 = 0$)

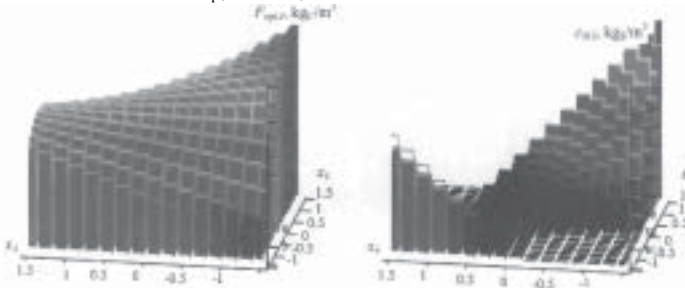


Fig. 4. $F_{opt,I}$ and $c_{Sf,I}$ vs. x_3 and x_4 ($x_1 = x_2 = 0$)

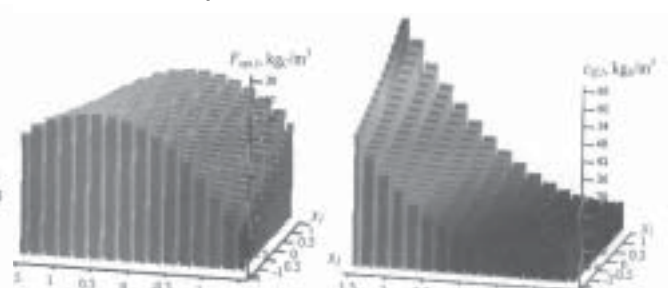


Fig. 7. $F_{opt,I}$ and $c_{Sf,I}$ vs. x_1 and x_3 ($x_2 = x_4 = 0$)

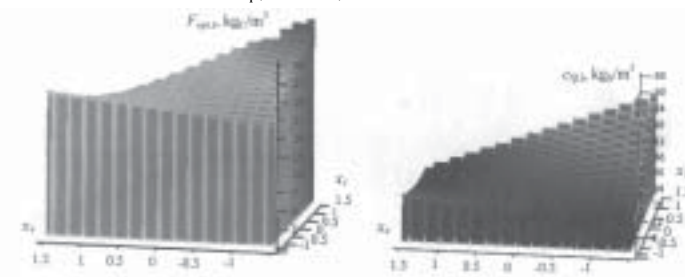


Fig. 5. $F_{opt,I}$ and $c_{Sf,I}$ vs. x_1 and x_4 ($x_2 = x_3 = 0$)

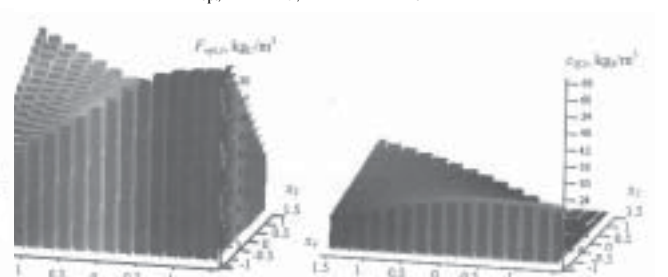


Fig. 8. $F_{opt,I}$ and $c_{Sf,I}$ vs. x_2 and x_4 ($x_1 = x_3 = 0$)

More simulations within the centre of experimental plan were performed in order to remove the non significant factors and interactions in the statistical models defined by eqs. (45) and (46), resulting in objective functions described by eqs. (51) and (52), where the functions $F_{opt,I}$, $c_{Sf,I}$ and $c_{Sf,II}$ are given by eqs. (53)-(55). Graphical representations in figures 3-8 show the variation of characteristic objective functions of the first stage of optimization procedure, $F_{opt,I}$ and $c_{Sf,I}$ with dimensionless process factors. The ranges of process factor values for which the objective functions are simultaneously optimized were selected based on these graphics. Optimal levels of dimensionless process factors and corresponding values of objective functions are summarized in table 4. Results depicted in figure 9 referring to characteristic ABE biosynthesis dynamics of B-FB bioreactor were obtained using values of process factors within the optimal ranges specified in table 4, i.e., $x_1 = -0.5$ ($c_{Sf,0} = 75 \text{ kg/m}^3$), $x_2 = 0.7$ ($F = 0.07 V_0$), $x_3 = 0$ ($c_{Sf} = 150 \text{ kg/m}^3$), and $x_4 = 0.4$ ($\tau_F = 12 \text{ h}$).

These optimal values of process factors were used as input fixed parameters (table 5) for the second stage of optimization procedure, where characteristic objective functions of B-FB-FBUP system, i.e., $F_{opt,II}(A_u, A_p, \tau_{UP})$ and $c_{Sf,II}(A_u, A_p, \tau_{UP})$, were optimized using a SORS model with 3 factors (table 6).

$$F_{opt,I}(x_1, x_2, x_3, x_4) = 18.275 - 1.048x_2 + 1.460x_3 - 2.180x_4 - 1.995x_1x_3 - 2.384x_1x_4 - 0.872x_2x_3 + F_{opt,0}(x_1, x_2, x_3, x_4) \quad (51)$$

$$c_{Sf,I}(x_1, x_2, x_3, x_4) = 19.657 + 3.027x_1 + 3.526x_2 + 14.698x_3 - 3.636x_4 + 3.097x_1x_3 - 4.519x_1x_4 + 4.713x_2x_3 + 4.589x_2x_4 - 45.3x_3x_4 + c_{Sf,0}(x_1, x_2, x_3, x_4) + c_{Sf,00}(x_1, x_2, x_3, x_4) \quad (52)$$

$$F_{opt,0}(x_1, x_2, x_3, x_4) = 2.350x_2x_4 - 2.353x_3x_4 + 2.336x_1x_2x_4 - 2.359x_1x_3x_4 + 2.379x_2x_3x_4 + 2.418x_1x_2x_3x_4 - 4.201(x_3^2 - 0.8) \quad (53)$$

$$c_{Sf,0}(x_1, x_2, x_3, x_4) = 4.941x_1x_2x_3x_4 + 1.060(x_1^2 - 0.8) - 1.839(x_2^2 - 0.8) + 7.310(x_3^2 - 0.8) \quad (54)$$

$$c_{Sf,00}(x_1, x_2, x_3, x_4) = 4.898x_1x_2x_3x_4 - 4.869x_1x_3x_4 + 4.625x_2x_3x_4 \quad (55)$$

Data summarized in table 6 emphasize that c_{SF} is almost invariant with the process factors (A_u , A_p , and τ_{UP}). In this case, the optimization problem consisted in maximizing the objective function $F_{opt,II}(A_u, A_p, \tau_p)$ defined by eq. (56). After removing the non significant factors and interactions in eq. (56), the statistical model described by eq. (57) was obtained.

$$F_{opt,II}(x_5, x_6, x_7) = \beta_0 + \sum_{j=5}^7 \beta_j x_j + \sum_{j=5}^7 \sum_{\substack{l=5 \\ l>j}}^7 \beta_{jl} x_j x_l + \sum_{j=5}^7 \beta_{jj} x_j^2 \quad (56)$$

$$F_{opt,II}(x_5, x_6, x_7) = 38.576 + 9.542x_6 - 1.852x_7 - 2.627x_6x_7 + 1.491(x_5^2 - 0.270) \quad (57)$$

Graphical representations in figures 10-12 show the variation of objective function $F_{opt,II}$ with dimensionless process factors. Based on these graphics, optimal values of process factors were determined as follows: $x_5=0$, $x_6=1.2$, and $x_7=-1.2$, corresponding to $A_u=40$ m², $A_p=48$ m², and $\tau_{PU}=18$ hr. Results depicted in figure 13 referring to characteristic ABE biosynthesis dynamics of B-FB-FBUP system were obtained using these optimal factor values.

Plots in figures 9 and 13 highlight that characteristic process dynamics of bioreactor are almost invariant with operation mode, i.e., B-FB (I) or B-FB-FBUP (II). However,

a slight increase in cellular content inside the bioreactor is observed for operating based on the solvent pervaporation. At the end of the process (100 h), a volume $V_{vf}=18.2$ m³ of aqueous solution of ABE solvents was accumulated in the collector of volatiles (fig. 13). Referring to ABE synthesis performances in terms of final butanol production ($m_{Bf,tot}$), which was estimated by eqs. (58) and (59), an amount almost 3 times higher was obtained using the integrated system II (table 7).

$$m_{Bf,I} = V_{f,I} C_{Bf,I} \quad (58)$$

$$m_{Bf,II} = V_{f,II} C_{Bf,II} + V_{vf} C_{Bvf} \quad (59)$$

Table 4
OPTIMAL LEVELS OF PROCESS FACTORS AND CORRESPONDING VALUES OF OBJECTIVE FUNCTIONS FOR ABE BIOSYNTHESIS IN B-FB SYSTEM

Dimensionless process factors			Objective functions	
Name	Symbol	Optimal values	$F_{opt,I}(x_1, x_2, x_3, x_4)$	$c_{SF,I}(x_1, x_2, x_3, x_4)$
Initial substrate concentration	x_1	-0.6 – -0.4	20.6 – 25.2 kg _C /m ³	4.6 – 12.5 kg _S /m ³
Feed flow rate	x_2	0.7 – 0.9		
Feed substrate concentration	x_3	-0.1 – 0.1		
Feed starting time	x_4	0.25 – 0.45		

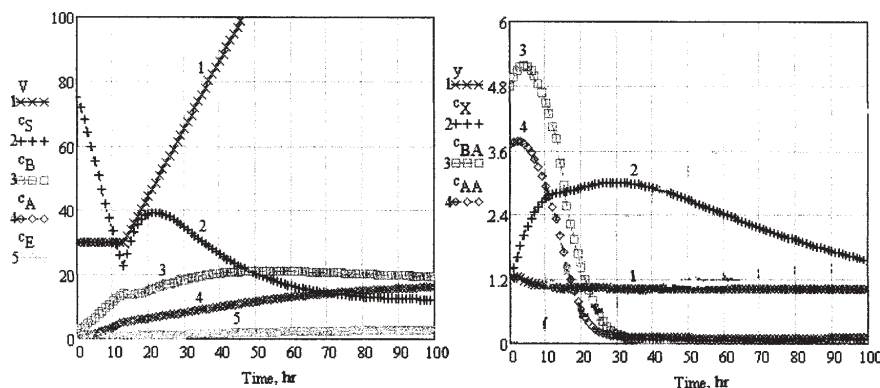


Fig. 9. Dynamics of ABE biosynthesis in B-FB system ($c_{S,0}=75$ kg/m³, $F=0.07V_0$, $c_{SF}=150$ kg/m³, $\tau_F=12$ h, $c_{X,0}=1.2$ kg/m³, $c_{B,0}=0.5$ kg/m³, $c_{A,0}=0.81$ kg/m³, $c_{E,0}=0.24$ kg/m³, $c_{BA,0}=4.78$ kg/m³, $c_{AA,0}=3.68$ kg/m³, $c_{CO_2,0}=c_{H_2,0}=0$ kg/m³, $y_0=1.2$, $V_0=30$ m³)

Type	Name	Symbol	Value	Unit
Manipulated	Ultrafiltration unit surface area	A_u	20, 40, 60	m ²
	Pervaporation unit surface area	A_p	15, 30, 45	m ²
	Ultrafiltration-pervaporation starting time	τ_{UP}	20, 30, 40	hr
Fixed	Glucose substrate concentration	$c_{S,0}$	75	kg/m ³
	Feed flow rate	F	$0.07V_0$	m ³ /hr
	Feed glucose concentration	c_{SF}	150	kg/m ³
	Feed starting time	τ_F	12	hr
	Exit flow rate	F_u	$0.07V_0$	m ³ /hr
	Biomass concentration	$c_{X,0}$	1.2	kg/m ³
	Butanol concentration	$c_{B,0}$	0.5	kg/m ³
	Acetone concentration	$c_{A,0}$	0.81	kg/m ³
	Ethanol concentration	$c_{E,0}$	0.24	kg/m ³
	Butyric acid concentration	$c_{BA,0}$	4.78	kg/m ³
	Acetic acid concentration	$c_{AA,0}$	3.68	kg/m ³
	Carbon dioxide concentration	$c_{CO_2,0}$	0	kg/m ³
	Hydrogen concentration	$c_{H_2,0}$	0	kg/m ³
	Marker concentration	y_0	1.2	-
Batch reactor volume	V_0	30	m ³	

Table 5
INPUT PARAMETERS FOR ABE BIOSYNTHESIS IN B-FB-FBUP SYSTEM

No.	x_5	x_6	x_7	x_5'	x_6'	x_7'	$F_{opt,II}$ (kgC/m ³)	$c_{SF,II}$ (kgS/m ³)
1	1	1	1	0.27	0.27	0.27	44.165	12.704
2	1	1	-1	0.27	0.27	0.27	53.319	12.601
3	1	-1	1	0.27	0.27	0.27	35.113	12.462
4	-1	1	1	0.27	0.27	0.27	44.172	12.727
5	-1	-1	1	0.27	0.27	0.27	26.662	12.175
6	-1	1	-1	0.27	0.27	0.27	52.336	12.575
7	1	-1	-1	0.27	0.27	0.27	29.029	11.808
8	-1	-1	-1	0.27	0.27	0.27	29.043	11.867
9	0	0	0	-0.73	-0.73	-0.73	37.791	12.368
10	1.225	0	0	0.77	-0.73	-0.73	37.785	12.377
11	-1.225	0	0	0.77	-0.73	-0.73	37.794	12.361
12	0	1.225	0	-0.73	0.77	-0.73	50.975	12.767
13	0	-1.225	0	-0.73	0.77	-0.73	25.812	11.985
14	0	0	1.225	-0.73	-0.73	0.77	34.563	12.462
15	0	0	-1.225	-0.73	-0.73	0.77	40.075	12.185

Table 6
SIMULATION MATRIX FOR ABE BIOSYNTHESIS IN
B-FB-FBUP SYSTEM USING SECOND-ORDER
RESPONSE SURFACE (SORS) MODEL

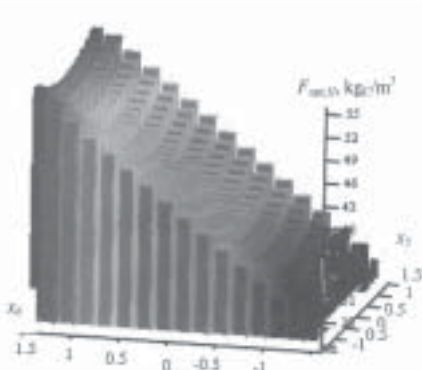


Fig. 10. $F_{opt,II}$ vs. x_5 and x_6 ($x_7=0$)

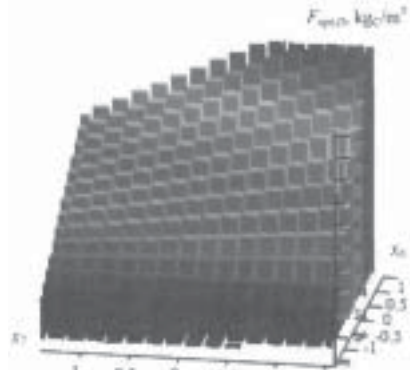


Fig. 11. $F_{opt,II}$ vs. x_6 and x_7 ($x_5=0$)

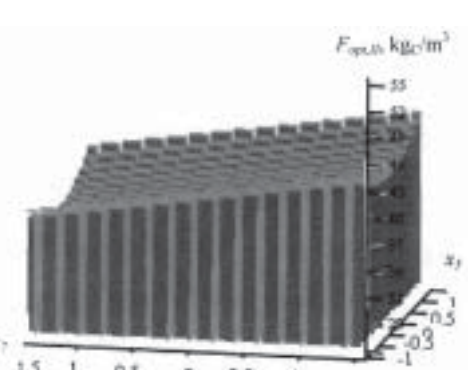


Fig. 12. $F_{opt,II}$ vs. x_5 and x_7 ($x_6=0$)

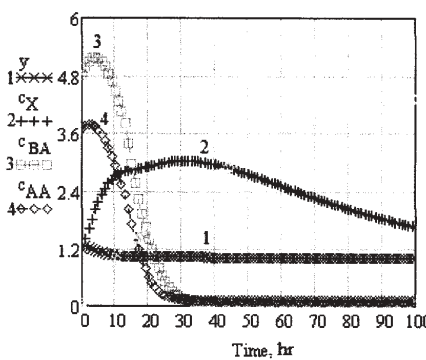
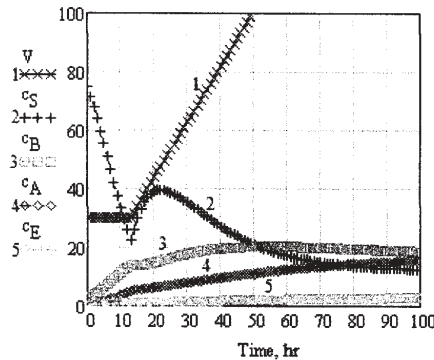
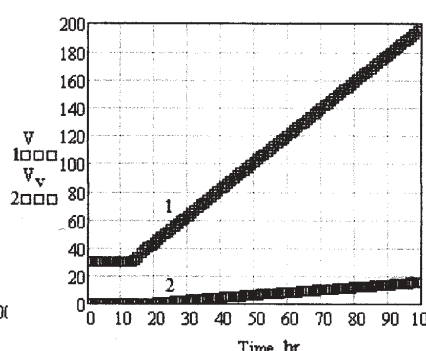
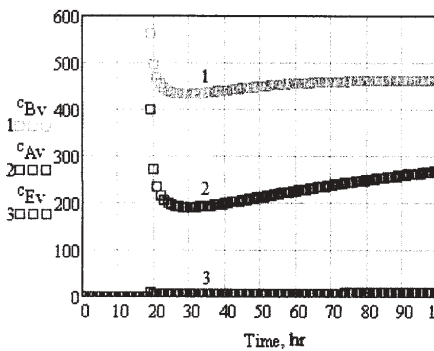


Fig. 13. Dynamics of ABE biosynthesis in B-FB-FBUP system ($A_u=40$ m², $A_p=48$ m², $\tau_{PU}=18$ hr, $c_{S,0}=75$ kg/m³, $F_u=F_p=0.07V_0$, $c_{SF}=150$ kg/m³, $\tau_F=12$ hr, $c_{X,0}=1.2$ kg/m³, $c_{B,0}=0.5$ kg/m³, $c_{A,0}=0.81$ kg/m³, $c_{E,0}=0.24$ kg/m³, $c_{BA,0}=4.78$ kg/m³, $c_{AA,0}=3.68$ kg/m³, $c_{CO_2,0}=c_{H_2,0}=0$ kg/m³, $y_0=1.2$, $V_0=30$ m³)



Operation mode	Bioreactor			Collector of volatiles			$m_{Bf,tot}$ (kg)
	V_f (m ³)	c_{Bf} (kg/m ³)	m_{Bf} (kg)	V_{vf} (m ³)	c_{Bvf} (kg/m ³)	m_{Bvf} (kg)	
B-FB (I)	216	20	4320	-	-	-	4320
B-FB-FBUP (II)	198	20	3960	18.2	460	8372	12332

Table 7
ABE BIOSYNTHESIS PERFORMANCES

Conclusions

A mathematical model was developed to describe the dynamics of ABE biosynthesis using *Clostridium acetobutylicum* culture in a batch (B)-fed batch (FB) bioreactor coupled with ultrafiltration (U) and pervaporation (P) units. An optimization case consisting

in maximizing the final ABE production and glucose substrate utilization was analyzed. Due to the large numbers of process factors, i.e., initial substrate concentration in the bioreactor ($c_{S,0}$), feed flow rate (F), feed substrate concentration (c_{SF}), starting time of feed (τ_F) and ultrafiltration-pervaporation (τ_{UP}), surface area of

ultrafiltration (A_u) and pervaporation (A_p) units, the optimization problem was solved in two successive stages.

In the first stage, the simulation of B-FB process using a SORS model with 4 factors ($c_{s,0}$, F , c_{sp} and τ_p) has aimed at identifying the optimal ranges of process factor values. Values of $c_{s,0}$, F , c_{sp} and τ_p within these optimal ranges were used as input data for the second optimization stage, wherein the B-FB-FBUP system was optimized using a SORS model with 3 factors (A_u , A_p and τ_{up}). The simulations of process dynamics emphasized that the substrate concentration in the final bioreactor was invariant with A_u , A_p and τ_{up} . Moreover, the final butanol production was about 3 times higher for the B-FB-FBUP system.

Acknowledgements: Ali A. A. Al Janabi expresses his gratitude to the Iraqi Ministry of Higher Education and Scientific Research as well as to the Al-Furat Al-AWSAT Technical University for their funding.

References

1. CHANG, W.L., Acetone-Butanol-Ethanol Fermentation by Engineered *Clostridium Beijerinckii* and *Clostridium Tyrobutyricum*, Ph.D. Thesis, Ohio State University, 2010.
2. GREEN, E.M., Curr. Opin. Biotechnol., **22**, 2011, p. 337.
3. KÓTAI, L., SZÉPVÖLGYI, J., SZILÁGYI, M., ZHIBIN, L., BAIQUAN, C., SHARMA, V., SHARMA, P.K., Liquid, Gaseous and Solid Biofuels - Conversion Techniques, Ed. Fang, Z., InTech, 2013, p. 199, <http://dx.doi.org/10.5772/52379>.
4. MARSZAŁEK, J., KAMINSKI, W., Concentration of Butanol-Ethanol-Acetone-Water using Pervaporation, Proceedings of ECOpole, **6**, no. 1, 2012, p. 31, DOI: 10.2429/proc.2012.6(1)003.
5. PETRIK, T., Combined Acetone, Butanol, Ethanol and Organic Acid Fermentation by a Degenerated Strain of *Clostridium Acetobutylicum* and Subsequent Esterification, Ph.D. Thesis, Michigan State University, 2011.
6. EZEJI, T.C., QURESHI, N., BLASCHEK, H.P., Curr. Opin. Biotechnol., **18**, 2007, p. 220.
7. JONES, D.T., WOODS, D.R., Microbiol. Rev., **50**, no. 4, 1986, p. 484.
8. LI, X., LI, Z.G., SHI, Z.P., Bioresources and Bioprocessing, 2014, p. 1, <http://www.bioresourcesbioprocessing.com/content/1/1/13>.
9. EVANS, P.J., WANG, H.Y., Appl. Environ. Microbiol., **54**, 1988, p. 1662.
10. ISHIZAKI, A., MICHIWAKI, S., CRABBE, E., KOBAYASHI, G., SONOMOTO, K., YOSHINO, S., J. Biosci. Bioeng., **87**, 1999, p. 352.
11. QURESHI, N., MADDOX, I.S., J. Ferment. Bioeng., **80**, 1995, p. 185.
12. EZEJI, T.C., QURESHI, N., BLASCHEK, H.P., Appl. Microbiol. Biotechnol., **63**, 2004, p. 653.
13. GROOT, W.J., VANDERLANS, R.M., LUYBEN, K.M., Appl. Microbiol. Biotechnol., **32**, 1989, p. 305.
14. YANG, X., TSAO, G.T., Biotechnol. Bioeng., **47**, 1995, p. 444.
15. GROBBEN, N.G., EGGINK, G., CUPERUS, F.P., HUIZING, H.J., Appl. Microbiol. Biotechnol., **39**, 1993, p. 494.
16. DONG, Z., LIU, G., LIU, S., LIU, Z., JIN, W., J. Membr. Sci., **450**, 2014, p. 38.
17. IZAK, P., SCHWARZ, K., RUTH, W., BAHL, H., KRAGL, U., Appl. Microbiol. Biotechnol., **78**, 2008, p. 597.
18. JEON, E.J., KIM, A.S., LEE, Y.T., Desalin. Water Treat., **48**, no. 1-3, 2012, p. 17.
19. LIU, G.P., WEI, W., WU, H., DONG, X.L., JIANG, M., JIN, W.Q., J. Membr. Sci., **373**, no. 1-2, 2011, p. 121.
20. MAI, N.L., KIM, S.H., HA, S.H., SHIN, H.S., KOO, Y.M., Korean J. Chem. Eng., **30**, no. 9, 2013, p. 1804.
21. MARSZAŁEK, J., WŁADYSŁAW, L.K., Chemical and Process Engineering **33**, no. 1, 2012, p. 131.
22. NIELSEN, D.R., PRATHER, K.J., Biotechnol. Bioeng., **102**, 2009, p. 811.
23. QURESHI, N., MEAGHER, M.M., HUANG, J., HUTKINS, R.W., J. Membr. Sci., **187**, 2001, p. 93.
24. SAKAKI, K., HABE, H., NEGISHI, H., IKEGAMI, T., Desalin. Water Treat., **34**, 2011, p. 290.
25. SETLHAKU, M., HEITMANN, S., GÓRAK, A., WICHMANN, R., Bioresource Technol., **136**, 2013, p. 102.
26. SANDU OHREAC, B., DOBRE, T., PÂRVULESCU, O.C., DANCIU, T.D., Rev. Chim. (Bucharest), **65**, no. 5, 2014, p. 582.
27. SANDU OHREAC, B., DOBRE, T., PÂRVULESCU, O.C., U.P.B. Sci. Bull., Series B, **76**, no. 4, 2014, p. 45.
28. VOLESKY, B., VOTRUBA, J., Modelling and Optimization of Fermentation Processes, Elsevier Science Publisher, 1992.
29. BAE, T.H., TAK, T.M., J. Membr. Sci., **264**, no. 1, 2005, p. 151.
30. VINCENT-VELA, M.C., CUARTAS-URIBE, B., ÁLVAREZ-BLANCO, S., LORA-GARCÍA, J., Desalination **284**, 2012, p. 14.
31. GÎJIU, C.L., DIMA, R., ISOPESCU, R.D., Rev. Chim. (Bucharest), **63**, no. 1, 2012, p. 60.
32. KABSCH-KORBUTOWICZ, M., URBANOWSKA, A., Environment Protection Engineering **36**, no. 1, 2010, p. 125.
33. MULLER, A., CHAUFER, B., MERIN, U., DAUFIN, G., Lait **83**, no. 2, 2003, p. 111.
34. VLADISAVLJEVIĆ, G.T., VUKOSAVLJEVIĆ, P., BUKVIĆ, B., J. Food Eng., **60**, no. 3, 2003, p. 241.
35. DOBRE, T., SANCHEZ MARCANO, J., Chemical Engineering - Modeling Simulation and Similitude, Wiley VCH, 2007

Manuscript received: 25.11.2014